Version of Record: https://www.sciencedirect.com/science/article/pii/S0022407320303228
Manuscript_77af064ed05198535cff2f8fde0de1e6

Calculated Spectroscopic Databases for the VAMDC portal: new molecules and improvements

C. Richard[a,*], V. Boudon[a], M. Rotger[b]

[a]*Laboratoire Interdisciplinaire Carnot de Bourgogne, UMR 6303 CNRS - Université Bourgogne Franche-Comté, 9 Av. A. Savary, BP 47870, F-21078 Dijon Cedex, France*
[b]*Groupe de Spectrométrie Moléculaire et Atmosphérique (GSMA), CNRS UMR 7331, Université de Reims Champagne-Ardenne, U.F.R. Sciences Exactes et Naturelles, Moulin de la Housse B.P. 1039, 51687 Reims Cedex 2, France*

Abstract

We report the current status of our calculated spectroscopic relational databases. They contain line lists for specific molecules, that result from recently published spectroscopic analyses. The two original databases, denoted MeCaSDa (CH_4) and ECaSDa (C_2H_4), have been greatly improved with the addition of new calculated lines. Then, five new databases, TFMeCaSDa (CF_4), SHeCaSDa (SF_6), GeCaSDa (GeH_4), RuCaSDa (RuO_4) and TFSiCasDa (SiF_4) were deployed based upon the same model. These databases are developed in the framework of the international consortium VAMDC (Virtual Atomic and Molecular Data Centre, http://vamdc.org) and are also part of the Dat@OSU project (http://dataosu.obs-besancon.fr).

Keywords: Spectroscopic databases, Calculated line lists, VAMDC

1. Introduction

Spectroscopic databases are essential tools for atmospheric, planetary and astrophysical sciences. All these disciplines perform radiative transfer calculations that rely on accurate molecular line lists containing line positions and intensities and line broadening coefficients. All these data rely on extensive laboratory studies, both experimental and theoretical. The huge variety of observational conditions, ranging for instance from very cold but dense (Titan, Saturn's main satellite [1]) to very hot ("hot-jupiter"-type exoplanets [2]) atmospheric environnements as well as the large diversity of implied molecular species imply that there exist no unique and definitive molecular spectroscopic database. Depending on the exact application, on can use several types of databases and compare them, each having their own advantages and drawbacks.

First, there are the very popular experimental or semi-experimental databases HITRAN [3] and GEISA [4] which are accurate (but require very regular updates) although not necessarily complete, depending on the species and spectral range. Recently, fully theoretical databases, based on quantum chemistry and variational calculations, appeared. The two most famous are ExoMol [5] and TheoReTS [6]. Their huge advantage is the spectral completeness, although the line position accuracy can still be lower for complex molecular polyads with strong interactions.

*Corresponding author
Email address: Cyril.Richard@u-bourgogne.fr (C. Richard)

Another intermediate type of database consists in calculated lines resulting from fits of line positions and / or intensities using experimental spectra and effective Hamiltonian and transition moments. These are accurate and complete for the rovibrational bands that have been investigated so far. We previously setup two of such databases for methane (CH_4) and ethylene (or ethene, C_2H_4) [7], based on analyses using the tensorial formalism and group theory methods used in the Dijon group [8, 9]. In the last years, we performed new laboratory studies concerning similar molecules with high symmetry: SF_6 [10] and CF_4 [11], which are strong greenhouse gases of industrial origin, GeH_4 [12], a species present in the atmospheres of Jupiter and Saturn, RuO_4 [13], a molecule of interest for nuclear industry and SiF_4 which is present in volcanic gases.

This paper thus intends to present the new data that have been updated and added in our Calculated Spectroscopic Databases (CaSDa) since the previous article of Ba et *al.* [7] in 2013 for methane (CH_4, MeCaSDa database) and ethene (C_2H_4, ECaSDa database). So far, the updated databases collect calculated spectroscopic data from the last accurate analyses of methane and ethene but also of germane (GeH_4, GeCaSDa database), carbon tetrafluoride (CF_4, TFMeCaSDa database), ruthenium tetroxide (RuO_4, RuCaSDa database), sulfur hexafluoride (SF_6, SHeCaSDa) and silicon tetrafluoride (SiF_4, TFSiCaSDa), through five new databases. These databases are all compatible with the XSAMS (XML Schema for Atoms, Molecules, and Solids) format adopted with the VAMDC European project [14–16] and are available on one hand from the online VAMDC portal (`http://portal.vamdc.org`) and from our webpage (`http://vamdc.icb.cnrs.fr`), in the HITRAN output format, on the other. Also, a special attention was given to our databases web pages and their many improvements are discussed in this paper.

2. Database generalities

Dijon spectroscopic databases include calculated line lists, including positions, intensities and full rovibrational transition labels, that are obtained from experimental spectroscopic analyses. Lines are assigned using the homemade SPVIEW (SPectrum VIEW) software [9] while Hamiltonians and dipole moments parameters are fitted with XTDS (eXTended spherical-top Data System) [9] software. The latter is also used to generate predictions that are included in the database.

2.1. Theoretical principles

The specificity of these databases is thus to contain only calculated line lists based on effective Hamiltonian and transition moment operators whose parameters were fitted using assigned experimental spectra. The databases thus contain full descriptions of molecular eigenstates, including all necessary quantum numbers.

The general idea for all molecules is to consider polyads, *i.e.* groups of interacting vibrational levels. A polyad can either be a single vibrational level (for instance an isolated fundamental level) or a more complex set of interacting levels like in the methane case [17]. Depending on the molecule and on the level of analysis that has been reached, different polyad schemes are used. Sometimes, several distinct polyad schemes can be used to deal with different spectral regions of the same molecule. Thus, in each database, one or several polyad schemes can be defined internally through a set of integers $(i_1, i_2, \ldots, i_N)$, where N is the number of distinct normal modes of the considered species ($N = 4$, 6 or 12 for XY_4, XY_6 and X_2Y_4 molecules,

respectively). Polyad number n, say P_n is thus defined automatically by all the sets of vibrational quantum numbers $(v_1, v_2, \ldots, v_N)$ that satisfy the relation:

$$n = \sum_{k=1}^{k=N} i_k v_k. \tag{1}$$

For instance, in the well-known case of the methane molecule (CH_4, MeCaSDa database), the approximate relation between its four normal mode frequencies, say $\nu_1 \simeq \nu_3 \simeq 2\nu_2 \simeq 2\nu_4$ leads to a single polyad scheme defined by $(i_1, i_2, i_3, i_4) = (2, 1, 2, 1)$ such that P_1 is the ν_2/ν_4 Dyad, P_2 is the $\nu_1/\nu_3/2\nu_2/2\nu_4/\nu_2 + \nu_4$ Pentad, *etc* [18].

The effective Hamiltonian operators is then decomposed into a series of contributions, one for each polyad, as:

$$\widetilde{\mathcal{H}} = \widetilde{\mathcal{H}}_{\{P_0\}} + \widetilde{\mathcal{H}}_{\{P_1\}} + \ldots + \widetilde{\mathcal{H}}_{\{P_k\}} + \ldots, \tag{2}$$

and the detailed writing of this operator, as well as that of the effective dipole moment (to calculate absorption line intensities) or effective polarizability (to calculate Raman scattering line intensities) has been described elsewhere, see for instance Refs. [8, 19, 20].

All calculations are performed in a symmetrized coupled rovibrational basis set:

$$\left|\Phi_{r\sigma}^{(C_r,\{i\},C_v,J,nC_r,C)}\right\rangle = \left|(\Psi_r^{(J,nC_r)} \otimes \Psi_v^{([s\}C_v)})_\sigma^{(C)}\right\rangle, \tag{3}$$

where all C symbols correspond to irreducible representations of the symmetry point group of the molecule. The rotational part $\Psi_r^{(J,nC_r)}$ depends on the rotational quantum number J and on a multiplicity index n that distinguishes levels within the same (J, C_r) block. The vibrational part $\Psi_v^{([s\}C_v)}$ consists in the coupling of elementary wave functions for each normal mode number k in the general form for component σ_k:

$$\left|\psi_{v_k\sigma_k}^{(l_k,n_kC_k)}\right\rangle = |v_k(l_k, n_kC_k, \sigma_k)\rangle, \tag{4}$$

where v_k is the associated vibrational quantum number, l_k is the vibrational angular momentum quantum number ($l_k = 0$ for non-degenerate modes).

The eigenvectors of $\widetilde{H}$ are decomposed over the above-defined initial rovibrational basis set:

$$\left|\Psi_\sigma^{(J,C,\alpha)}\right\rangle = \sum_{\{i\},C_r,C_v} C_{\{i\},C_r,C_v}^{\alpha} \left|\Phi_{r\sigma}^{(C_r,\{i\},C_v,J,nC_r,C)}\right\rangle. \tag{5}$$

Here, α numbers eigenvectors within the same (J, C) block, in increasing eigenenergy order. Our databases contain this full decomposition through the full list of $C_{\{i\},C_r,C_v}^{\alpha}$ coefficients.

2.2. Querying CaSDa through dedicated webpages

A refactoring effort was performed to our database website in order to provide a better user-friendly interface. First, all databases are accessible through the main website page at the following url: `http://vamdc.icb.cnrs.fr`. It is now possible to retrieve line-by-line spectroscopic parameters list in the 160-character HITRAN2004 format [21], as well as cross-section data that are computed by the binned sum of intensities. These latter are given in an easy two-columns output format that allows a more flexible use. The retrieved data are also plotted as shown in Figure 1. Our databases do not include isotopic abundances (or, saying this differently, isotopic abundances are all set to 100 %). It is important to note that the broadening parameters of all databases are presently set to zero, since we do not yet provide calculated values (although it is one of our future projects).

As seen in Table 1, MeCaSDa contains more than ten million lines. As a consequence, the execution time of the query can be quite long if the user tries to retrieve the whole base at once.

2.3. Querying CaSDa through the VAMDC portal

All databases can be queried from the online VAMDC portal (`http://portal.vamdc.eu/vamdc_portal/home.seam`) in the same way than described in our previous paper [7]. As default, data are provided in a single XML document: the XSAMS format ouput. Though, our group has developed a tool that convert XSAMS format to HITRAN2004 output. This tool is now available on the VAMDC portal and can be selected after the user queried the database. However, XSAMS format provides much more information than one can retrieve with the HITRAN file but specific tools are needed to parse data.

Due to the large amount of data in MeCaSDa, TFMeCaSDa and SHeCaSDa, the result is truncated at 100 000 lines. This issue is currently under consideration and could be fixed using asynchronous tasks in a future update of VAMDC.

2.4. CaSDa in the Dat@OSU project

Dat@OSU[1] is a platform aimed to provide a description of digital data sets from scientific research in the form of metadata records. Our bases are accessible through the following url: `https://dataosu.obs-besancon.fr/coll/4`, where each molecule is referenced in an information sheet that provides a description of which data are calculated.

3. Spectroscopic data updates

3.1. CH_4

Methane is one of the most important molecules contributing to the opacity of the atmospheres of exoplanets and brown dwarfs [25]. The strong transition of methane at 3 μm completely dominates the spectrum of brown darfs at 1600 K and is still identifiable at 1800 K [26]. However, high-temperature spectroscopic data cannot be extrapolated from low-temperature atmospheric data such as HITRAN and GEISA because they fail to reproduce high J rovibrational and hot band transitions involving highly excited vibrational levels.

In order to produce a precise synthetic line list of methane suitable for the high temperature applications, successive global analyses of high temperature emission spectra of methane were recently performed by Amyay *et al.* in Refs. [27] and [17]. The first study was devoted to the Dyad band system (1100–1500 cm^{-1}) of methane including the cold band and three hot bands up to the Tetradecad such as $\delta_n = \pm 1$, n being the polyad number. The use of high temperature emission spectra (1400 K) rather than the usual low or moderate temperature absorption spectra allows significant improvements in the observed data. Indeed, the assignments of the Dyad cold band lines and the well-known hot bands were extended rotationally up to about $J = 30$. Such data bring important information over the couplings terms, in particular for Coriolis type interactions. As a result of this study, 14 415 assigned transitions were fitted together with the previously observed data using 1096 effective parameters.

As for the first analysis of higher states, the second study focuses on the Pentad system with $\delta_n = \pm 2$. The high temperature (620–1715 K) emission spectra of the ν_3 C−H stretching region of $^{12}CH_4$ was considered in this work. 6 067 assignments of vibration-rotation line positions belonging to the ν_3 cold band and related hot bands up to $J = 30$ have been successfully achieved. The global effective model was extended in this study to the 6th order in the case of the first three

[1] `https://dataosu.obs-besancon.fr`

Table 1: Rovibrational transitions in MeCaSDa for $^{12}CH_4$ and $^{13}CH_4$ (see ref. [7] for polyad definitions). The polyad sheme is described by the $(i_1; i_2; ...; i_N)$ multiplet as explained in section 2.1.

Transitions	Nb. dipolar	Nb. Raman	Dipolar wavenumber cm^{-1}	Dipolar intensity cm^{-1}/(molecule cm^{-2})	Raman wavenumber cm^{-1}	Raman intensity arbitrary unit
$^{12}CH_4$						
Scheme 1 (2,1,2,1)						
$P_0 - P_0$	2 116	0	0 – 310	2×10^{-40} – 8×10^{-25}		
$P_1 - P_0$	22 017	19 064	831 – 1951	1×10^{-35} – 2×10^{-20}	671 – 2076	2×10^{4} – 4×10^{18}
$P_1 - P_1$	53 311	0	0 – 800	8×10^{-41} – 8×10^{-25}		
$P_2 - P_0$	55 751	72 954	1971 – 3591	8×10^{-31} – 2×10^{-19}	1842 – 3685	3×10^{-1} – 2×10^{20}
$P_2 - P_1$	358 980	0	490 – 2450	8×10^{-36} – 4×10^{-22}		
$P_2 - P_2$	700 884	0	0 – 1307	8×10^{-41} – 2×10^{-27}		
$P_3 - P_0$	149 685	140 906	3187 – 5161	8×10^{-31} – 4×10^{-21}	3123 – 5179	2×10^{4} – 2×10^{17}
$P_3 - P_1$	387 058	373 495	1861 – 3937	8×10^{-31} – 4×10^{-22}	1696 – 3804	2×10^{4} – 4×10^{17}
$P_3 - P_2$	2 384 563	0	335 – 2895	8×10^{-36} – 1×10^{-24}		
$P_4 - P_0$	311 965	0	4476 – 6773	8×10^{-31} – 2×10^{-21}		
$P_4 - P_1$	759 273	0	3173 – 5282	8×10^{-31} – 2×10^{-23}		
$P_4 - P_2$	802 484	2 865 111	1933 – 3959	8×10^{-31} – 8×10^{-25}	1459 – 4097	2×10^{4} – 9×10^{14}
$P_4 - P_3$	6 646 051	0	372 – 2975	8×10^{-36} – 3×10^{-27}		
$^{13}CH_4$						
Scheme 1 (2,1,2,1)						
$P_0 - P_0$	1 222	0	0 – 253	8×10^{-49} – 8×10^{-25}		
$P_1 - P_0$	13 025	0	901 – 1865	8×10^{-39} – 4×10^{-19}		
$P_1 - P_1$	31 525	0	0 – 694	3×10^{-62} – 8×10^{-25}		
$P_2 - P_0$	49 475	14 636	2057 – 3478	4×10^{-40} – 2×10^{-19}	2325 – 3219	2×10^{1} – 2×10^{20}
$P_2 - P_1$	247 325	0	439 – 2307	8×10^{-49} – 4×10^{-22}		
$P_3 - P_0$	12 188	0	3605 – 4742	8×10^{-32} – 8×10^{-21}		
Total	12 988 898	3 486 166				

polyads $n <= 3$, and to the 5th order for the Octad and the Tetradecad systems. Thus 1306 effective parameters were fitted to the complete set of assigned data now including 16 475 064 transitions using a global approach. This study is part of the ANR e-PYTHEAS project [2][2] which combines theoretical and experimental work with exoplanet modeling applications.

Finally, no Raman data have been added since the last update in 2013 and the entirety of the synthetic line list is summarized in Table 1.

Figure 2 shows a comparison of the MeCaSDa cross-sections data using a logarithmic scale, at a resolution of 1 cm^{-1}, with ExoMol [5] and TheoReTS [6], where much of the data give a very good agreement. However, for one particular weak region around 800 cm^{-1}, there are larger differences that can be explained by a lack of hot bands and high J value data. The HITRAN 2016 [3] database contains less hot band and high-J lines and thus gives discrepancies in the low-intensity regions between polyads. But it should be noticed that the HITEMP database was very recently updated thanks to the TheoReTS lines [28]. Figure 3 exhibits the same comparison in the region of 1200–1400 cm^{-1}, but using a linear intensity scale. Figure 4 displays the distribution of the lower sates of all MeCaSDa transitions; when more lower states are present, higher temperature spectrum calculation can be performed.

[2] `htpp://e-pytheas.cnrs.fr`

3.2. C_2H_4

$^{12}C_2H_4$ is a naturally occurring molecule playing a role in the atmosphere of the Earth as a tropospheric pollutant [29]. It is also produced in the petrochemical industry and by automobile exhaust emissions. The molecule is also of astrophysical interest because the emission of the Asymptotic Giant Branch stars is partly affected by ethene which has been detected in the outer shell of IRC+10216 [30] and CRL618 [31].

A new global frequency and intensity analysis of the infrared tetrad of $^{12}C_2H_4$ (600–1500 cm^{-1}), performed by Alkadrou *et al.* in 2016 [32], produced a new set of parameters that generate 96 756 synthetic lines in the ν_{10}, ν_7, ν_4 and ν_{12} bands of $^{12}C_2H_4$. These lines have been introduced in the ECaSDa database using only one polyad scheme contrary to the choice that has been made in the previous update. This new calculated line list is more reliable than the previous one, especially concerning line intensities; in the near future, we intend to re-introduce the 3000 cm^{-1} C–H stretching region, that as been removed here, thanks to a new spectrum analysis which is currently in progress.

Table 2 shows the total number of transitions with the wavenumber and intensity ranges currently available. Figure 5 compares calculated absorption cross-sections between different databases.

Finally, it is important to mention that the HITRAN file output given by our database is quite different from the one provided by the HITRAN online website, as far as quantum numbers are concerned. While in the latter the molecule is listed in the Group 1 of asymmetric rotors for quanta identification, we made a different choice to conform to our formalism and fully describe the vibrational state, as shown in Table 3.

Table 2: Rovibrational transitions in ECaSDa. The polyad sheme is described by the $(i_1; i_2; ...; i_N)$ multiplet as explained in section 2.1.

Transitions	Nb. dipolar	Dipolar wavenumber cm^{-1}	Dipolar intensity cm^{-1}/(molecule cm^{-2})
$^{12}C_2H_4$			
Scheme 1 (0,0,0,1,0,0,1,0,0,1,0,1)			
$P_1 - P_0$	96 756	620 – 1525	$2\times10^{-45} - 8\times10^{-20}$
Total	96 756		

Table 3: Part of a output line showing notation differences between our database and the official HITRAN output for one transition. First line is the output of our database while the second one was extracted on HITRAN online.

```
EcaSDA: 381  620.057966 ... 1025.06720.000.00000000000100000B2u000000000000A g 24 B2u 10 ...
HITRAN: 381  620.057948 ... 1025.06720.760.000000            V7         GROUND 24  6 18 ...
```

4. New molecules

4.1. CF_4

Carbon tetrafluoride or tetrafluoromethane (CF_4) is a powerful greenhouse gaz mainly of anthropogenic origin that contributes to the global warming. It is very stable due to the strength of its carbonfluorine bonds and has an estimated lifetime of more than 50 000 years [33, 34]. For these reasons, CF_4 has been included in the Kyoto Protocol [35–37].

In order to produce a suitable synthetic line list for radiative transfer atmospheric models, successive global analyses of $^{12}CF_4$ rovibrational bands and pure rotation spectrum were recently performed by Carlos *et al.* [38] and Boudon *et al.* [39]. The first analysis was dedicated to the study of 17 rovibrational bands, but, contrary to methane (CH_4), CF_4 has no well-defined polyad structure yet and two different polyad schemes were used. The second study, focused on the rotational lines in the $\nu_3 = 1$ state, uses a third scheme.

The TFMeCaSDa (Tetra-Fluoro-Methane Calculated Spectroscopic Database) was then generated using these recent data and Table 4 summarizes the addition of 258 208 transitions using this global approach.

Table 4: Rovibrational transitions in TFMeCaSDa. The polyad sheme is described by the (i_1; i_2; ...; i_N) multiplet as explained in section 2.1.

Transitions	Nb. dipolar	Dipolar wavenumber cm^{-1}	Dipolar intensity cm^{-1}/(molecule cm^{-2})
$^{12}CF_4$			
Scheme 1 (0,2,6,3)			
$P_6 - P_0$	39 086	1230 – 1305	8×10^{-25} – 8×10^{-22}
$P_3 - P_0$	15 149	583 – 682	8×10^{-27} – 8×10^{-24}
$P_8 - P_2$	33 430	1231 – 1330	8×10^{-25} – 1×10^{-20}
Scheme 2 (3,0,4,2)			
$P_6 - P_0$	3 408	1231 – 1330	8×10^{-25} – 1×10^{-21}
Scheme 3 (0,0,2,1)			
$P_6 - P_0$	167 135	1199 – 1331	8×10^{-31} – 4×10^{-27}
Total	258 208		

Figure 6 displays the distribution of the lower sates of all TFMeCaSDa transitions; this illustrates the recent addition of hot band lines in this base.

4.2. SF_6

Sulfur hexafluoride is a powerful greenhouse gas of industrial origin. Its lifetime in the atmosphere is very long, around 3200 years, while its global warming potential (*ca.* 23900) is huge, compared to CO_2 [40–43]. Hence it is very important to study this molecule as its concentration should be monitored and reduced, as stated by the Kyoto protocol [44]. As a

heavy molecule, it possesses a very dense infrared spectrum, with many low-lying vibrational states, leading to the generation of a lot of hot bands at room temperature [45]. For this reason, our group, in collaboration with experimentalists (especially at the AILES Beamline of the Soleil Synchrotron facility [46]) undertook in the past years a systematic spectroscopic study of a large number of rovibrational bands over a wide spectral range [10, 47–49]. Although not finished, this work allows to setup a database, SHeCaSDa (Sulfur Hexafluoride Calculated Spectroscopic Database), containing cold and hot bands in the strongly absorbing ν_4 and ν_3 regions, for the four isotopologues that are present in natural-abundance SF_6. The database also includes Raman lines for some fundamental bands, but only with relative line intensities, since there exist no absolute intensity measurements with this technique. Therefore, Table 5 presents these results with the addition of 491 500 transitions. These calculated lines have been introduced using six different schemes for the four isotopologues (including the very rare $^{36}SF_6$ that could be studied recently [50]).

Table 5: Rovibrational transitions in SHeCaSDa. The polyad sheme is described by the (i_1; i_2; ...; i_N) multiplet as explained in section 2.1.

Transitions	Nb. dipolar	Nb. Raman	Dipolar wavenumber cm^{-1}	Dipolar intensity cm^{-1}/(molecule cm^{-2})	Raman wavenumber cm^{-1}	Raman intensity arbitrary unit
$^{32}SF_6$						
Scheme 1 (2,1,3,0,0,0)						
$P_1 - P_0$		42 983			600 – 687	2×10^{18} – 6×10^{20}
$P_2 - P_0$		7 861			773 – 775	2×10^{17} – 3×10^{21}
$P_4 - P_2$		11 797			770 – 773	2×10^{17} – 2×10^{20}
$P_3 - P_0$	53 996		935 – 957	8×10^{-24} – 2×10^{-20}		
$P_4 - P_1$	32 371		932 – 959	8×10^{-24} – 8×10^{-22}		
$P_5 - P_2$	11 473		937 – 949	8×10^{-24} – 4×10^{-22}		
Scheme 2 (0,0,0,2,0,1)						
$P_2 - P_0$	14 941		593 – 637	8×10^{-24} – 1×10^{-21}		
$P_3 - P_1$	34 575		593 – 637	8×10^{-24} – 2×10^{-22}		
$P_1 - P_0$	62 895		320 – 374	8×10^{-29} – 4×10^{-26}		
Scheme 3 (0,4,0,2,1,0)						
$P_1 - P_0$		59 842			475 – 562	2×10^{18} – 4×10^{20}
$P_3 - P_1$	121 841		932 – 964	8×10^{-24} – 1×10^{-21}		
Scheme 4 (0,0,2,0,1,0)						
$P_1 - P_0$		17 987			772 – 773	3×10^{17} – 2×10^{20}
$P_3 - P_1$	3 935		599 – 630	8×10^{-24} – 3×10^{-23}		
$^{33}SF_6$						
Scheme 5 (0,0,1,0,0,0)						
$P_1 - P_0$	1 620		937 – 941	2×10^{-22} – 2×10^{-20}		
$^{34}SF_6$						
Scheme 5 (0,0,1,0,0,0)						
$P_1 - P_0$	1 620		928 – 933	2×10^{-22} – 2×10^{-20}		
Scheme 6 (0,0,0,1,0,0)						
$P_1 - P_0$	3 920		600 – 624	2×10^{-23} – 1×10^{-21}		
$^{36}SF_6$						
Scheme 5 (0,0,1,0,0,0)						
$P_1 - P_0$	7 843		908 – 920	1×10^{-21} – 2×10^{-20}		
Total	351 030	140 470				

Figure 7 displays the distribution of the lower sates of all SHeCaSDa transitions; this illus-

trates the recent addition of hot band lines in this base.

4.3. GeH_4

In 1978, Fink *et al.* [51] report the presence of germane (GeH_4) in Jupiter's atmosphere. This detection is followed by some line identifications of the molecule in the atmosphere of Saturn by Noll *et al.* [52], ten years later, in 1988. In both cases, detection was made for transitions in the ν_3 band which is of great interest for modeling the 4.5–5.0 μm region in the two giant planets atmosphere. A first complete analysis of the ν_1/ν_3 stretching dyad region for all natural five isotopologues ($^{70}GeH_4$, $^{72}GeH_4$, $^{73}GeH_4$, $^{74}GeH_4$ and $^{76}GeH_4$) was recenlty performed by Boudon *et al.* [53]. They produced an accurate model of the positions and intensities covering the range 1929 cm^{-1} – 2266 cm^{-1}. Thus a set of 32 378 calculated lines has been collected in the new GeCaSDa (Germane Calculated Spectroscopic Database) database and is summarized in Table 6.

Table 6: Rovibrational transitions in GeCaSDa. The polyad sheme is described by the (i_1; i_2; ...; i_N) multiplet as explained in section 2.1.

Transitions	Nb. dipolar	Dipolar wavenumber cm^{-1}	Dipolar intensity cm^{-1}/(molecule cm^{-2})
$^{70}GeH_4$			
Scheme 1 (1,0,1,0)			
$P_1 - P_0$	6417	1930 – 2266	8×10^{-24} – 4×10^{-19}
$^{72}GeH_4$			
Scheme 1 (1,0,1,0)			
$P_1 - P_0$	6459	1930 – 2265	8×10^{-24} – 4×10^{-19}
$^{73}GeH_4$			
Scheme 1 (1,0,1,0)			
$P_1 - P_0$	6472	1930 – 2265	8×10^{-24} – 4×10^{-19}
$^{74}GeH_4$			
Scheme 1 (1,0,1,0)			
$P_1 - P_0$	6512	1929 – 2265	8×10^{-24} – 4×10^{-19}
$^{76}GeH_4$			
Scheme 1 (1,0,1,0)			
$P_1 - P_0$	6518	1929 – 2265	8×10^{-24} – 4×10^{-19}
Total	32 378		

Figure 8 shows a comparison of the GeCaSDa and TheoReTS [6] databases for the $^{74}GeH_4$ isotopologue of this molecule.

4.4. RuO_4

Ruthenium tetroxide (RuO_4) is another tetrahedral molecule but with a heavier central atom, that is ruthenium. Since this latter is a fission product of uranium, the relatively volatile ruthenium tetroxide can be used as a marker during a severe nuclear reactor accident with air ingress [54]. Natural abundance of ruthenium has seven isotopologues: ^{97}Ru, ^{98}Ru, ^{99}Ru, ^{100}Ru, ^{101}Ru, ^{102}Ru and ^{104}Ru but it also exists under the form of two radioactive isotpologues: ^{103}Ru and ^{106}Ru. Therefore, accurate line list for all existant isotopologues of ruthenium tetroxide are required by remote sensing applications dedicated to monitor the molecule concentration.

New investigations were thus carried out by Reymond-Laruinaz *et al.* [55] and by Auwera *et al.* [56] in order to analyse the strong ν_3 stretching fundamental region around 920 cm^{-1}, respectively in position and intensity. In the first study, the five main natural isotopologues have been then measured and fitted while the two minor and the two radioactive ones were extrapolated. At the end of the second analysis which consisted in high-resolution measurements of individual rovibrational line intensities of a pure $^{102}Ru^{16}O_4$ and extrapolation to the other isotpologues, a new list of line positions and intensities was generated. This list of 30 205 lines was included in a new database named RuCaSDa (Ruthenium tetroxide Calculated Spectroscopic Database) and informations about this new database are shown in Table 7. Also, as RuO_4 has no entry in HITRAN database and is not planned for inclusion in the immidiate future, it was decided to set the flag value 99 for the molecule ID field.

4.5. SiF_4

Silicon tetrafluoride (SiF_4) is a trace component of fumarole gases on volcanoes [57] and is thus adapted to remote IR spectroscopy using its strong absorption band ν_3 at 1032 cm^{-1}. This molecule has been identified in this way among other species in the volcanic plumes of Etna [57, 58], Popocatépetl [59–62] or Satsuma-Iwojima [63] volcanoes. It has even been suggested that silicon tetrafluoride should be present on Io, the highly volcanic moon of Jupiter [64]. A correct and quantitative detection thus requires a good knowledge of the molecule's infrared spectrum, both in terms of line positions and line intensities. We could recently preform a detailed study of several bands of SiF_4, including a first estimate of absolute intensities in the ν_3 band [65], allowing to build the TFSiCaSDa database (Tetra-Fluoro Silane Calculated Spectroscopic Database). Detailed information is given in Table 8. As of RuO_4, this molecule gets ID 99 in the HITRAN notation, as it is not included in this database.

5. Discussion

Each molecule is associated to one database based on a set of fourteen database tables as illustrated in Figure 9. All our databases have the same structure and are compatible with the standardized XSAMS format adopted within the VAMDC European project. For more detailed information, please refer to Ref. [7] that describe the structure point by point.

The choice of getting involved in the VAMDC project is motivated by the need for modern databases to comply with a standard. Indeed, the database ecosystem is made up of too many projects using their own structure, format, units and so on, often depending on historical reasons. It is therefore difficult for the users who do not belong to the same research field and who do not

speak the same "language" to correctly find their needs in this jungle. So far, VAMDC format is still perfectible, especially for databases containing a huge set of data (which is generally the case for calculated ones), but these issues are under consideration and should be fixed in the future as explained in section 2.3.

We have previously said that our calculated spectroscopy databases contain information that are not included in the HITRAN file output. Consequently we are currently working on the ability of retrieving full eigenvector composition through a user friendly web interface. Such data are of great interest in various applications such as line-mixing and collisional coefficients calculations that are essential in radiative transfer models used by atmospheric and planetary sciences.

For users who want to calculate spectra at temperatures other than 296, it is intended to provide a webpage computing partition functions for all databases, as a generalization of what was previously presented for methane in Ref. [66]. This work will be presented in a future article.

Comparison of our results with different databases, as shown in Figures 2, 3, 5 and 8, is very consistent and gives high confidence in the accuracy of our calculated data (this is particularly true in Figure 3 where TheoReTS and MeCaSDa perfectly match). Inclusion of hot bands is however highly needed in many cases in order to better describe faintest part of spectra.

Finally, as seen with the CH_4 molecule, in section 3.1, some of our databases contain Raman lines, but only with relative line intensities. Although these data are accessible through our webpage, we have deliberately postponed the inclusion of Raman bands. We intend to perform this by using calculated polarizability values is order to have consistent absolute Raman intensities (which are very difficult to measure experimentally). This will be presented in a future article.

6. Conclusion

We have presented here an important update of our previously existing calculated spectroscopic databases, as well as new databases built on the same model. This represents a major progress since the initial paper on this topic in 2013 [7]. Concerning future developments, besides those mentioned in previous section concerning Raman spectra and interface improvements, we, of course, intend to continue to update the databases regularly, by including the results of new spectrum analyses.

The main needs for new experimental data that would help to perform new fits and add new calculated lines are mostly related to the "new" and heavy molecules in this series of databases: GeH_4, RuO_4, SiF_4, but also SF_6 and CF_4. Requirements concern combination and overtone bands in order to be able to simulate more hot bands, even for the last two cited molecules for which this has started but is still incomplete.

Moreover, we have projects to introduce new databases for other molecules which are presently under study. This includes some more tetrahedral (SiH_4) and octahedral molecules (SeF_6, UF_6, ...), but also some molecules with lower symmetry like C_{3v} symmetric-tops for which we have built specific programs based on tensorial formalism [67–69]. This could include CH_3D and trioxane ($C_3H_6O_3$).

Aknowledgments

The authors wish to thanks the VAMDC consortium and the OSU THETA of Franche-Comté Bourgogne and Dat@OSU project for their support. We also gratefully acknowledges the CNRS-

ANR e-PYTHEAS project (contract ANR-16-CE31-0005-03) and the Université Bourgogne Franche-Comté (UBFC) for financial support.

References

[1] M. Hirtzig, B. Bézard, E. Lellouch, A. Coustenis, C. de Bergh, P. Drossart, A. Campargue, V. Boudon, V. Tyuterev, P. Rannou, T. Cours, S. Kassi, A. Nikitin, D. Mondelain, S. Rodriguez, S. L. Mouélic, Titan's surface and atmosphere from Cassini/VIMS data with updated methane opacity, Icarus 226 (2013) 470–486.

[2] A. Coustenis, V. Boudon, A. Campargue, R. Georges, V. G. Tyuterev, Exo-planetary high-temperature hydrocarbons by emission and absorption spectroscopy (the e-pytheas project), in: European Planetary Science Congress, Vol. 11, 2017.

[3] I. E. Gordon, L. S. Rothman, C. Hill, R. V. Kochanova, Y. Tan, P. F. Bernath, M. Birk, V. Boudon, A. Campargue, K. V. Chance, B. J. Drouin, J.-M. Flaud, R. R. Gamache, J. T. Hodges, D. Jacquemart, V. I. Perevalov, A. Perrin, K. P. Shine, M.-A. H. Smith, J. Tennyson, G. C. Toon, H. Tran, V. G. Tyuterev, A. Barbe, A. Csaszar, M. V. Devi, T. Furtenbacher, J. J. Harrison, A. Jolly, T. Johnson, T. Karman, I. Kleiner, A. A. Kyuberis, J. Loos, O. M. Lyulin, S. T. Massie, S. N. Mikhailenko, N. Moazzen-Ahmadi, H. S. P. Müller, O. V. Naumenko, A. V. Nikitin, O. L. Polyansky, M. Rey, M. Rotger, S. Sharpe, K. Sung, E. Starikova, S. A. Tashkun, J. V. Auwera, G. Wagner, J. Wilzewski, P. Wcisło, S. Yu, E. J. Zak, The HITRAN2016 Molecular Spectroscopic Database, J. Quant. Spectrosc. Radiat. Transfer 203 (2017) 3–69.

[4] N. Jacquinet-Husson, R. Armante, N. A. Scott, A. Chedin, L. Crepeau, C. Boutammine, A. Bouhdaoui, C. Crevoisier, V. Capelle, C. Boonne, N. Poulet-Crovisier, A. Barbe, D. C. Benner, V. Boudon, L. R. Brown, J. Buldyreva, A. Campargue, L. H. Coudert, V. M. Devi, M. J. Down, B. J. Drouin, A. Fayt, C. Fittschen, J. M. Flaud, R. R. Gamache, J. J. Harrison, C. Hill, O. Hodnebrog, S. M. Hu, D. Jacquemart, A. Jolly, E. Jimenez, N. N. Lavrentieva, A. W. Liu, L. Lodi, O. M. Lyulin, S. T. Massie, S. Mikhailenko, H. S. P. Mueller, O. V. Naumenko, A. Nikitin, C. J. Nielsen, J. Orphal, V. I. Perevalov, A. Perrin, E. Polovtseva, A. Predoi-Cross, M. Rotger, A. A. Ruth, S. S. Yu, K. Sung, S. A. Tashkun, J. Tennyson, V. I. G. Tyuterev, J. V. Auwera, B. A. Voronin, A. Makie, The 2015 edition of the GEISA spectroscopic database, J. Mol. Spectrosc. 327 (2016) 31–72.

[5] J. Tennyson, S. N. Yurchenko, A. F. Al-Refaie, E. J. Barton, K. L. Chubb, P. A. Coles, S. D. and. M. N. Gorman, C. Hill, A. Z. Lam, L. Lodi, L. K. McKemmish, Y. Na, A. Owens, O. L. Polyansky, T. Rivlin, C. Sousa-Silva, D. S. Underwood, A. Yachmenev, E. Zak, The ExoMol database: Molecular line lists for exoplanet and other hot atmospheres, Journal of Molecular Spectroscopy 327 (2016) 73–94.

[6] M. Rey, A. V. Nikitin, Y. L. Babikov, V. G. Tyuterev, TheoReTS – An information system for theoretical spectra based on variational predictions from molecular potential energy and dipole moment surfaces, J. Mol. Spectrosc. 327 (2016) 138–158.

[7] Y. A. Ba, C. Wenger, R. Surleau, V. Boudon, M. Rotger, L. Daumont, D. A. Bonhommeau, V. G. Tyuterev, M.-L. Dubernet, MeCaSDa and ECaSDa: Methane and ethene calculated spectroscopic databases for the virtual atomic and molecular data centre, Journal of Quantitative Spectroscopy and Radiative Transfer 130 (2013) 62–68.

[8] V. Boudon, J.-P. Champion, T. Gabard, M. Loëte, M. R. C. Wenger, Spherical top theory and molecular spectra, in: M. Quack, F. Merkt (Eds.), Handbook of High-Resolution Spectroscopy, Vol. 3, Wiley, Chichester, West Sussex, United Kingdom, 2011, pp. 1437–1460.

[9] C. Wenger, V. Boudon, M. Rotger, M. Sanzharov, J.-P. Champion, XTDS and SPVIEW: graphical tools for the analysis and simulation of high-resolution molecular spectra, Journal of Molecular Spectroscopy 251 (1) (2008) 102–113.

[10] M. Faye, V. Boudon, M. Loëte, P. Roy, L. Manceron, The high overtone and combination levels of SF_6 revisited at doppler-limited resolution: A global effective rovibrational model for highly excited vibrational states, J. Quant. Spectrosc. Radiat. Transfer 190 (2017) 38–47.

[11] M. Carlos, O. Gruson, C. Richard, V. Boudon, M. Rotger, X. Thomas, C. Maul, C. Sydow, A. Domanskaya, R. Georges, P. Souard, O. Pirali, M. Goubet, P. Asselin, T. R. Huet, High-resolution spectroscopy and global analysis of cf_4 rovibrational bands to model its atmospheric absorption, J. Quant. Spectrosc. Radiat. Transfer 201 (2017) 75–93.

[12] V. Boudon, T. Grigoryan, F. Philipot, C. Richard, F. Kwabia Tchana, L. Manceron, A. Rizopoulos, J. Vander Auwera, T. Encrenaz, Line positions and intensities for the ν_3 band of 5 isotopologues of germane for planetary applications, J. Quant. Spectrosc. Radiat. Transfer 205 (2018) 174–183.

[13] J. Vander Auwera, S. Reymond-Laruinaz, V. Boudon, D. Doizi, L. Manceron, Line intensity measurements and analysis in the ν_3 band of ruthenium tetroxide, J. Quant. Spectrosc. Radiat. Transfer 204 (2018) 103–111.

[14] M. Dubernet, D. Humbert, R. Clark, R. E. Ralchenko Yu, D. Schultz, XSAMS: XML schema for Atomic, Molecular and Solid Data, Dubernet ML, Humbert D, Ralchenko Yu, editors. Version 0.1 (2009).

[15] M.-L. Dubernet, V. Boudon, J. Culhane, M. Dimitrijevic, A. Fazliev, C. Joblin, F. Kupka, G. Leto, P. Le Sidaner, P. Loboda, et al., Virtual atomic and molecular data centre, Journal of Quantitative Spectroscopy and Radiative Transfer 111 (15) (2010) 2151–2159.

[16] M.-L. Dubernet, B. Antony, Y.-A. Ba, Y. L. Babikov, K. Bartschat, V. Boudon, B. Braams, H.-K. Chung, F. Daniel, F. Delahaye, et al., The virtual atomic and molecular data centre (vamdc) consortium, Journal of Physics B: Atomic, Molecular and Optical Physics 49 (7) (2016) 074003.

[17] B. Amyay, A. Gardez, R. Georges, L. Biennier, J. Vander Auwera, C. Richard, V. Boudon, New investigation of the ν_3 C–H stretching region of $^{12}CH_4$ through the analysis of high temperature infrared emission spectra, J. Chem. Phys. 148 (2018) 134306.

[18] V. Boudon, M. Rey, M. Loëte, The vibrational levels of methane obtained from analyses of high-resolution spectra, J. Quant. Spectrosc. Radiat. Transfer 98 (2006) 394–404.

[19] V. Boudon, J.-P. Champion, T. Gabard, M. Loëte, F. Michelot, G. Pierre, M. Rotger, C. Wenger, M. Rey, Symmetry-adapted tensorial formalism to model rovibrational and rovibronic spectra of molecules pertaining to various point groups, J. Mol. Spectrosc. 228 (2004) 620–634.

[20] M. Rey, V. Boudon, M. Loëte, Tensorial development of the rovibronic Hamiltonian and transition moment operators for octahedral molecules, J. Mol. Struct. 599 (2001) 125–137.

[21] L. S. Rothman, D. Jacquemart, A. Barbe, D. Chris Benner, M. Birk, L. R. Brown, M. R. Carleer, J. C. Chackerian, K. Chance, L. H. Coudert, V. Dana, V. M. Devi, J. M. Flaud, R. R. Gamache, A. Goldman, J. M. Hartmann, K. W. Jucks, A. G. Maki, J. Y. Mandin, S. T. Massie, J. Orphal, A. Perrin, C. P. Rinsland, M. A. H. Smith, J. Tennyson, R. N. Tolchenov, R. A. Toth, J. Vander Auwera, P. Varanasi, G. Wagner, The hitran 2004 molecular spectroscopic database, J. Quant. Spectrosc. Radiat. Transfer 96 (2005) 139–204.

[22] E. Jourdanneau, F. Chaussard, R. Saint-Loup, T. Gabard, H. Berger, The methane Raman spectrum from 1200 to 5500 cm^{-1}: A first step toward temperature diagnostic using methane as a probe molecule in combustion systems, J. Mol. Spectrosc. 233 (2005) 219–230.

[23] E. Jourdanneau, T. Gabard, F. Chaussard, R. Saint-Loup, H. Berger, E. Bertseva, F. Grisch, Cars methane spectra: Experiments and simulations for temperature diagnostic purposes, J. Mol. Spectrosc. 246 (2007) 167–179.

[24] F. Grisch, E. Bertseva, M. Habiballah, E. Jourdanneau, F. Chaussard, R. Saint-Loup, T. Gabard, H. Berger, CARS spectroscopy of CH_4 for implication of temperature measurements in supercritical LOX/CH_4 combustion, Aerospace Science and Technology 11 (2007) 48–54.

[25] M. R. Swain, G. Vasisht, G. Tinetti, The presence of methane in the atmosphere of an extrasolar planet, Nature 452 (2008) 329–331.

[26] A. Borysov, J.-P. Champion, U. G. Jørgensen, C. Wenger, Towards simulation of high temperature methane spectra, Mol. Phys. 100 (2002) 3585–3594.

[27] B. Amyay, M. Louviot, O. Pirali, R. Georges, J. Vander Auwera, V. Boudon, Global analysis of the high temperature infrared emission spectrum of $^{12}CH_4$ in the dyad (ν_2/ν_4) region, The Journal of Chemical Physics 144 (2) (2016) 024312.

[28] R. J. Hargreaves, I. E. Gordon, M. Rey, A. V. Nikitin, V. G. Tyuterev, R. V. Kochanov, L. S. Rothman, An accurate, extensive, and practical line list of Methane for the HITEMP Database, Astrophys. J. Supp. Ser. 247 (2020) 55.

[29] S. Sawada, T. Totsuka, Natural and anthropogenic sources and fate of atmospheric ethylene, Atmospheric Environment (1967) 20 (5) (1986) 821–832.

[30] A. Betz, Ethylene in IRC+ 10216, The Astrophysical Journal 244 (1981) L103–L105.

[31] J. Cernicharo, A. M. Heras, J. R. Pardo, A. Tielens, M. Guélin, E. Dartois, R. Neri, L. Waters, Methylpolyynes and small hydrocarbons in CRL 618, The Astrophysical Journal Letters 546 (2) (2001) L127.

[32] A. Alkadrou, M.-T. Bourgeois, M. Rotger, V. Boudon, J. Vander Auwera, Global frequency and intensity analysis of the $\nu_{10}/\nu_7/\nu_4/\nu_{12}$ band system of $^{12}C_2H_4$ at 10 μm using the D_{2h} top data system, Journal of Quantitative Spectroscopy and Radiative Transfer 182 (2016) 158–171.

[33] A. Ravishankara, S. Solomon, A. A. Turnipseed, R. Warren, Atmospheric lifetimes of long-lived halogenated species, Science 259 (1993) 194–199.

[34] R. A. Morris, T. M. Miller, A. Viggiano, J. F. Paulson, S. Solomon, G. Reid, Effects of electron and ion reactions on atmospheric lifetimes of fully fluorinated compounds, Journal of Geophysical Research: Atmospheres 100 (1995) 1287–1294.

[35] J. Harnisch, D. de Jager, J. Gale, O. Stobbe, Halogenated compounds and climate change: Future emission levels and reduction costs, Environ. Sci. & Pollut. Res. 9 (2002) 369–374.

[36] J. Harnisch, N. Höhne, Comparison of emissions estimates derived from atmospheric measurements with national estimates of HFCs, PFCs and SF_6, Environ. Sci. & Pollut. Res. 9 (2002) 315–320.

[37] V. Boudon, J.-P. Champion, T. Gabard, G. Pierre, M. Loëte, C. Wenger, Spectroscopic tools for remote sensing of greenhouse gases CH_4, CF_4 and SF_6, Environ. Chem. Lett. 1 (2003) 86–91.

[38] M. Carlos, O. Gruson, C. Richard, V. Boudon, M. Rotger, X. Thomas, C. Maul, C. Sydow, A. Domanskaya, R. Georges, et al., High-resolution spectroscopy and global analysis of CF_4 rovibrational bands to model its atmo-

spheric absorption, Journal of Quantitative Spectroscopy and Radiative Transfer 201 (2017) 75–93.
[39] V. Boudon, M. Carlos, C. Richard, O. Pirali, Pure rotation spectrum of CF_4 in the $\nu_3 = 1$ state using thz synchrotron radiation, Journal of Molecular Spectroscopy (2018).
[40] D. T. Ho, P. Schlosser, Atmospheric SF_6 near a large urban area, Geophys. Res. Lett. 27 (11) (2000) 1679–1682.
[41] T. Reddmann, R. Ruhnke, W. Kouker, Three dimentional model simulations of SF_6 with mesospheric chemistry, J. Geophys. Res. 106 (2001) 14525–14537.
[42] M. A. K. Khalil, R. A. Rasmussen, J. A. Culbertson, J. M. Prins, E. P. Grimsrud, M. J. Shearer, Atmospheric perfluorocarbons, Environ. Sci. Technol. 37 (2003) 4358–4361.
[43] C. P. Rinsland, C. Boone, R. Nassar, K. Walker, P. Bernath, E. Mathieu, R. Zander, J. C. McConnell, L. Chiou, Trends of HF, HCl, CCl_2F_2, CCl_3F, $CHClF_2$ (HFC-22), and SF_6 in the lower stratosphere from Atmospheric Chemistry Experiment (ACE and Atmospheric Trace Molecule Spectroscopy (ATMOS) measurements near 30°N latitude, Geophys. Res. Lett. 32 (2005) L16S03–1–5.
[44] J. Reilly, M. Mayer, J. Harnisch, The Kyoto Protocol and non-CO_2 greenhouse gases and carbon sinks, Environmental Modeling and Assessment 7 (2002) 217–229.
[45] V. Boudon, G. Pierre, Rovibrational spectroscopy of sulphur hexafluoride: A review, in: S. G. Pandalai (Ed.), Recent research developments in molecular spectroscopy, Vol. 1, Transworld Research Network, Trivandrum, India, 2002, pp. 25–55.
[46] J.-B. Brubach, L. Manceron, M. Rouzières, O. Pirali, D. Balcon, F. Tchana, V. Boudon, M. Tudorie, T. Huet, A. Cuisset, P. Roy, Performance of the AILES THz-infrared beamline on SOLEIL for high resolution spectroscopy, AIP Conference Proceeding 1214 (2010) 81–84.
[47] M. Faye, A. L. Ven, V. Boudon, L. Manceron, P. Asselin, P. Soulard, F. Kwabia Tchana, P. Roy, High-resolution spectroscopy of difference and combination bands of SF_6 to elucidate the $\nu_3 + \nu_1 - \nu_1$ and $\nu_3 + \nu_2 - \nu_2$ hot band structures in the ν_3 region, Mol. Phys. 112 (2014) 2504–2514.
[48] M. Faye, V. Boudon, M. Loëte, P. Roy, L. Manceron, Observation and analysis of the SF_6 $\nu_2 + \nu_4 - \nu_5$ band: Improved parameters for the $\nu_5 = 1$ state, J. Mol. Spectrosc. 325 (2016) 35–41.
[49] M. Faye, L. Manceron, P. Roy, V. Boudon, M. Loëte, First analysis of the $\nu_3 + \nu_5$ combination band of sf_6 observed at doppler-limited resolution and effective model for the $\nu_3 + \nu_5 - \nu_5$ hot band, J. Mol. Spectrosc. 348 (2018) 37–42.
[50] M. Faye, L. Manceron, P. Roy, V. Boudon, M. Loëte, First high resolution analysis of the ν_3 band of the $^{36}SF_6$ isotopologue, J. Mol. Spectrosc. 346 (2018) 23–26.
[51] U. Fink, H. P. Larson, R. R. Treffers, Germane in the atmosphere of Jupiter, Icarus 34 (1978) 344–354.
[52] K. S. Noll, R. Knacke, T. Geballe, A. Tokunaga, Evidence for germane in Saturn, Icarus 75 (1988) 409–422.
[53] V. Boudon, T. Grigoryan, F. Philipot, C. Richard, F. K. Tchana, L. Manceron, A. Rizopoulos, J. Vander Auwera, T. Encrenaz, Line positions and intensities for the ν_3 band of 5 isotopologues of germane for planetary applications, Journal of Quantitative Spectroscopy and Radiative Transfer (2017) 174–183.
[54] J. Holm, H. Glänneskog, C. Ekberg, Deposition of RuO_4 on various surfaces in a nuclear reactor containment, Journal of Nuclear Materials 392 (2009) 55–62.
[55] S. Reymond-Laruinaz, V. Boudon, L. Manceron, L. Lago, D. Doizi, Infrared spectroscopy of ruthenium tetroxide and high-resolution analysis of the ν_3 band, Journal of Molecular Spectroscopy 315 (2015) 46–54.
[56] J. Vander Auwera, S. Reymond-Laruinaz, V. Boudon, D. Doizi, L. Manceron, Line intensity measurements and analysis in the ν_3 band of ruthenium tetroxide, Journal of Quantitative Spectroscopy and Radiative Transfer 204 (2018) 103–111.
[57] P. Francis, C. Chaffin, A. Maciejewski, C. Oppenheimer, Remote determination of SiF_4 in volcanic plumes: A new tool for volcano monitoring, Geophys. Res. Lett. 23 (1996) 249–242.
[58] E. Nicotra, M. Viccaro, C. Ferlito, R. Cristofolini, Influx of volatiles into shallow reservoirs at Mt. Etna volcano (Italy) responsible for halogen-rich magmas, Eur. J. Mineral. 22 (2010) 121–138.
[59] W. Stremme, I. Ortega, C. Siebe, M. Grutter, Gas composition of Popocatépelt volcano between 2007 and 2008: FTIR spectroscopic measurements of an explosive event during quiescent degassing, Earth Plan. Sc. Lett. 301 (2011) 502–510.
[60] W. Stremme, A. Krueger, R. Harig, M. Grutter, Volcanic SO_2 and SiF_4 visualization using 2-D thermal emission spectroscopy – Part 1: Slant-columns and their ratios, Atmos. Meas. Tech. 5 (2012) 275–288.
[61] A. Krueger, W. Stremme, R. Harig, M. Grutter, Volcanic SO_2 and SiF_4 visualization using 2-D thermal emission spectroscopy – Part 2: Wind propagation and emission rates, Atmos. Meas. Tech. 6 (2013) 47–61.
[62] N. Taquet, W. Stremme, M. Grutter, J. Baylón, A. Bezanilla, B. Schiavo, C. Rivera, R. Campion, T. Boulesteix, A. Nieto-Torres, R. Espinasa-Pereña, T. Blumenstock, F. Hase, Variability in the gas composition of the Popocatépelt volcano plume, Front. Earth Sci. 7 (2019) 114–1–114–14.
[63] T. Mori, M. Sato, Y. Shimoike, K. Notsu, High SiF_4/HF ratio detected in Satsuma-Iwojima volcano's plume by remote FT-IR onservation, Earth Plan. Sp. 54 (2002) 249–256.
[64] L. Schaefer, B. Fegley Jr., Silicon tetrafluoride on Io, Icarus 179 (2005) 252–258.
[65] V. Boudon, L. Manceron, C. Richard, High-resolution spectroscopy and analysis of the ν_3, ν_4 and $2\nu_4$ of sif_4 in

natural isotopic abundance, in preparation (2020).

[66] C. Wenger, J. Champion, V. Boudon, The partition sum of methane at high temperature, Journal of Quantitative Spectroscopy and Radiative Transfer 109 (16) (2008) 2697–2706.

[67] A. E. Hilali, V. Boudon, M. Loëte, Spectroscopy of XY_3Z (C_{3v}) molecules: A tensorial formalism adapted to the $O(3) \supset C_{\infty v} \supset C_{3v}$ group chain, J. Mol. Spectrosc. 234 (2005) 113–121.

[68] A. E. Hilali, V. Boudon, M. Loëte, Development of the Hamiltonian and transition moment operators of symmetric top molecules using the $O(3) \supset C_{\infty v} \supset C_{3v}$ group chain, J. Mol. Spectrosc. 234 (2005) 176–181.

[69] A. E. Hilali, C. Wenger, V. Boudon, M. Loëte, C_{3v} Top Data System (C_{3v}TDS) software for spectrum simulation of XY_3Z symmetric-top molecules using the $O(3) \supset C_{\infty v} \supset C_{3v}$ group chain, J. Quant. Spectrosc. Radiat. Transfer 111 (2010) 1305–1315.

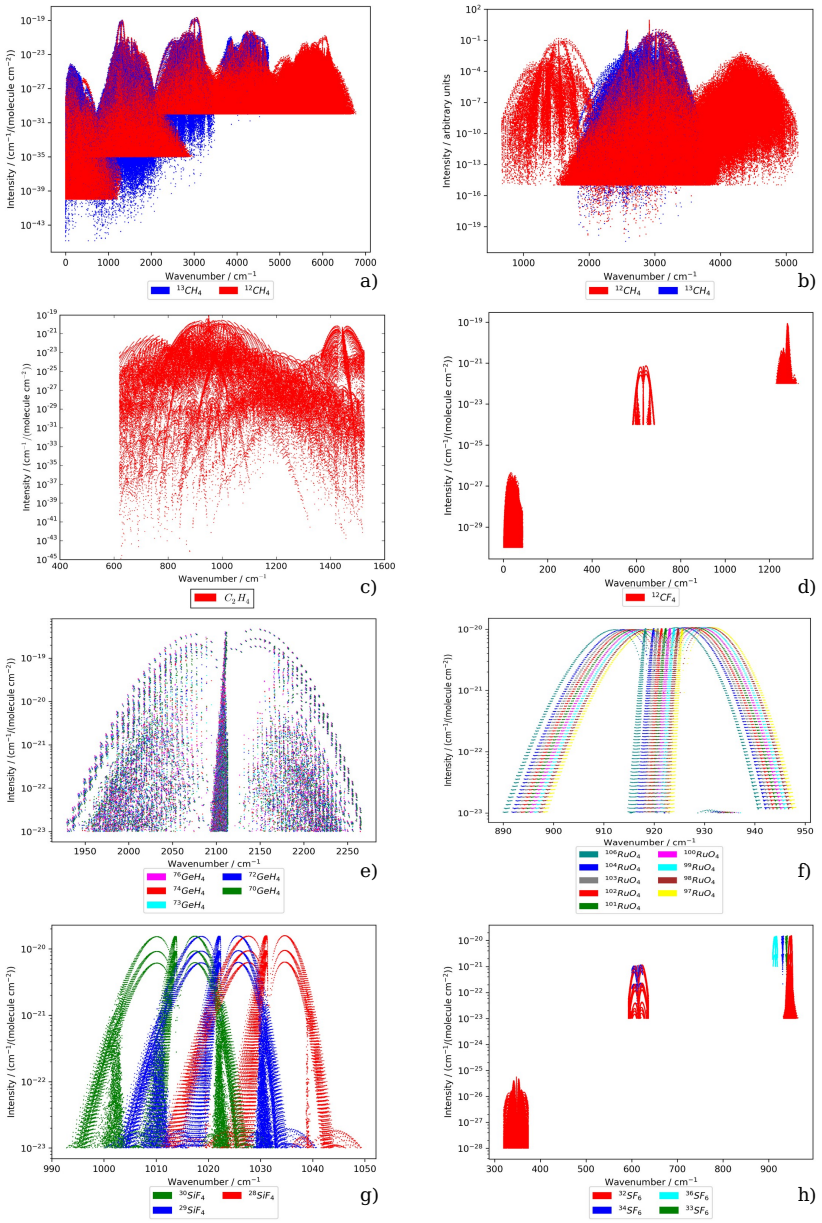

Figure 1: Graphical representation of the database contents. a) $^{12}CH_4$ and $^{13}CH_4$ infrared absorption lines in MeCaSDa. b) $^{12}CH_4$ and $^{13}CH_4$ Raman lines in MeCaSDa; these lines were included previously for use in optical diagnostic applications in flames [22–24]. c) C_2H_4 infrared absorption lines in ECaSDa. d) CF_4 infrared absorption lines in TFMeCaSDa. e) GeH_4 infrared absorption lines in GeCaSDa, with 5 isotopologues. f) RuO_4 infrared absorption lines in RuCaSDa, with 9 isotopologues. g) SiF_4 infrared absorption lines in TFSiCaSDa, with 3 isotopologues. h) SF_6 infrared absorption lines in SHeCaSDa, with 3 isotopologues.

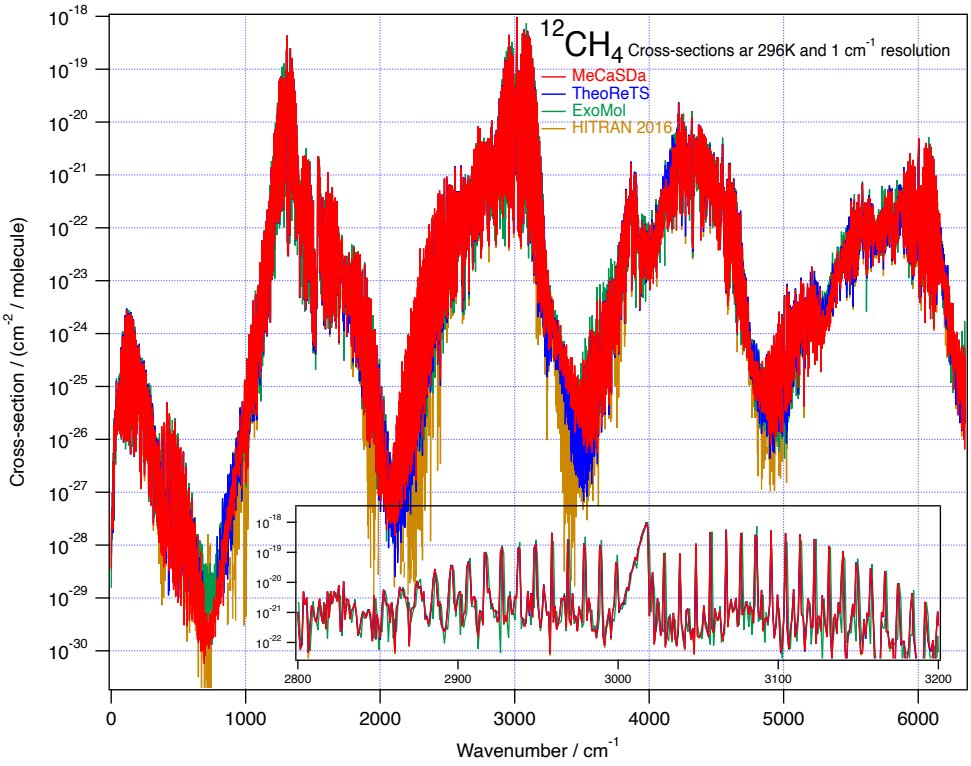

Figure 2: Calculated cross-sections (logarithmic scale) at a temperature of 296 K and a resolution of 1 cm^{-1} for the $^{12}CH_4$ molecule. Data are compared to ExoMol (green curve), TheoReTS (blue curve) and HITRAN 2016 (brown curve) showing a good match except in the 800 cm^{-1} region where a lack of hot bands and high J value data explain these discrepancies. The insert shows the region of the ν_3 stretching fundamental.

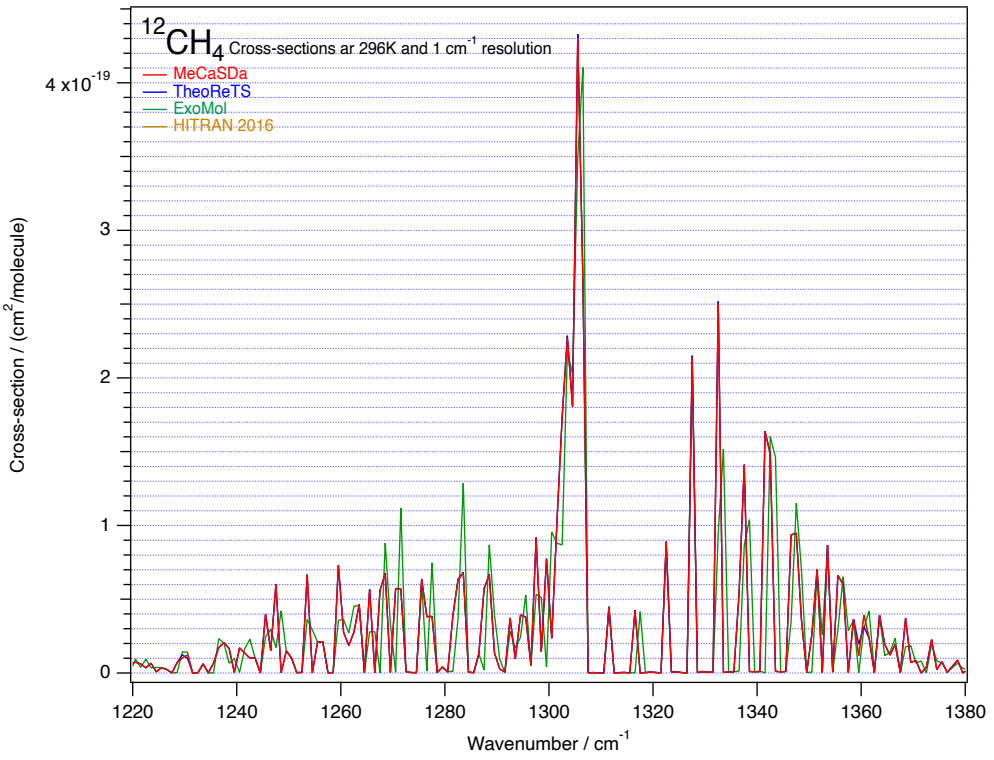

Figure 3: Zoom on the 1200–1400 cm^{-1} region of the calculated cross-sections of $^{12}CH_4$ (linear scale). The TheoReTS database contains more hot band lines, but it is almost identical to MeCaSDa in this spectral region at room temperature. This is also the case for HITRAN 2016. ExoMol is less accurate for line positions.

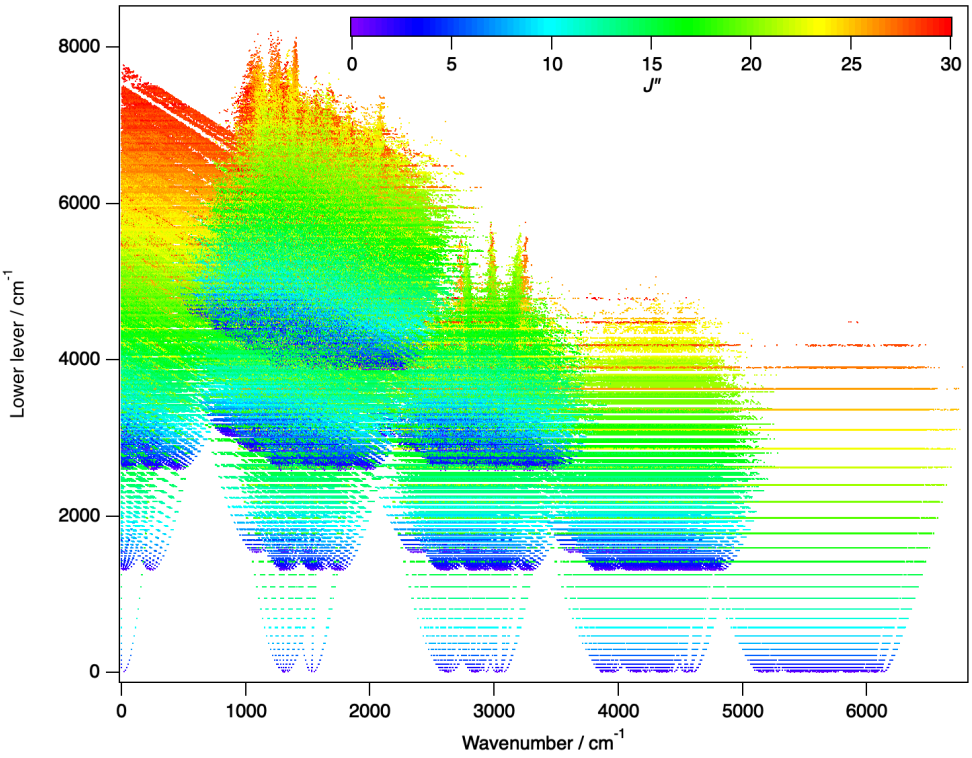

Figure 4: Representation of the lower level wavenumber for all transitions present in the MeCaSDa database. Colors are used to display the lower state rotational quantum number value, J''.

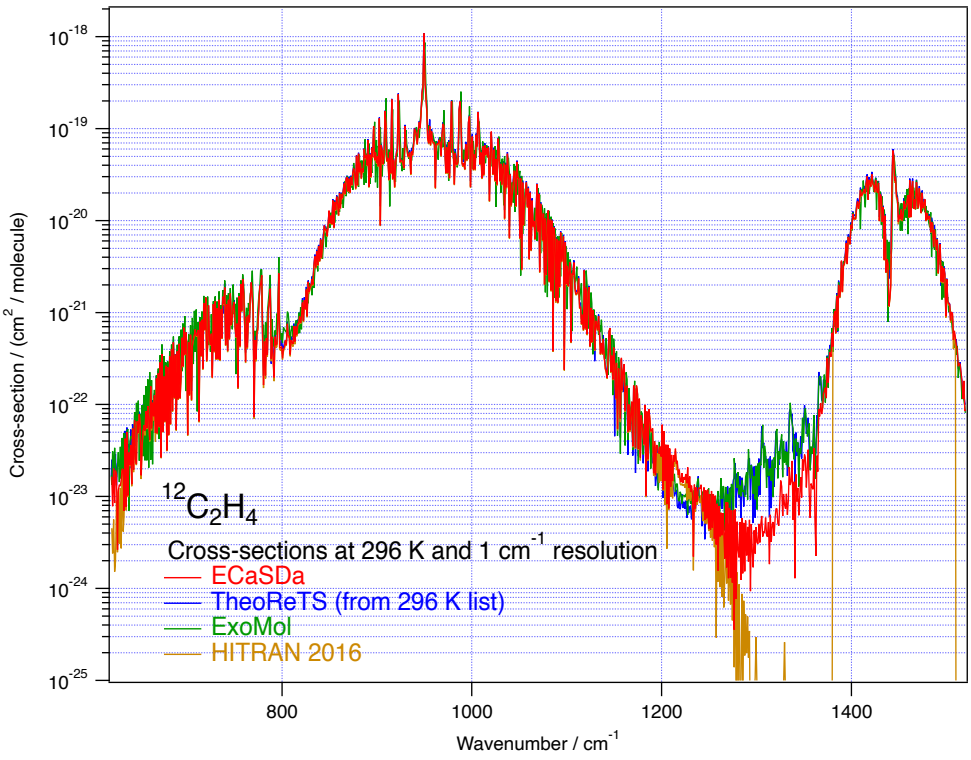

Figure 5: Calculated cross-sections at a temperature of 296 K and a resolution of 1 cm^{-1} for the $^{12}C_2H_4$ molecule. Discrepancies are visible between 1200 and 1400 cm^{-1}. In this region, where no measures were taken, ECaSDa datatabase is an high J extrapolation.

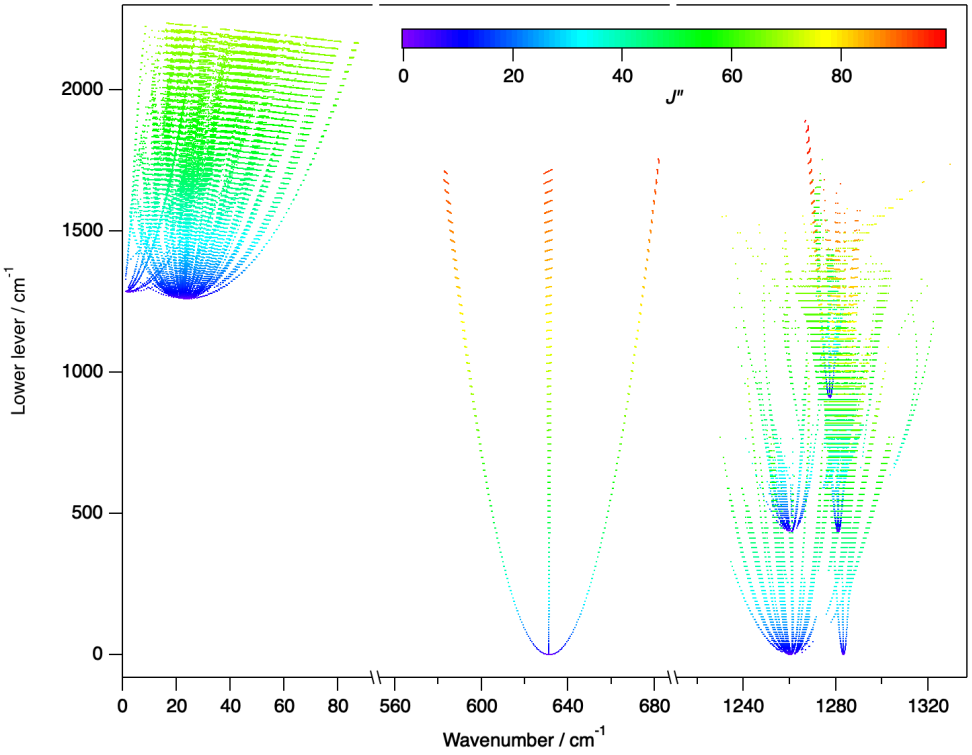

Figure 6: Representation of the lower level wavenumber for all transitions present in the TFMeCaSDa database. Colors are used to display the lower state rotational quantum number value, J''.

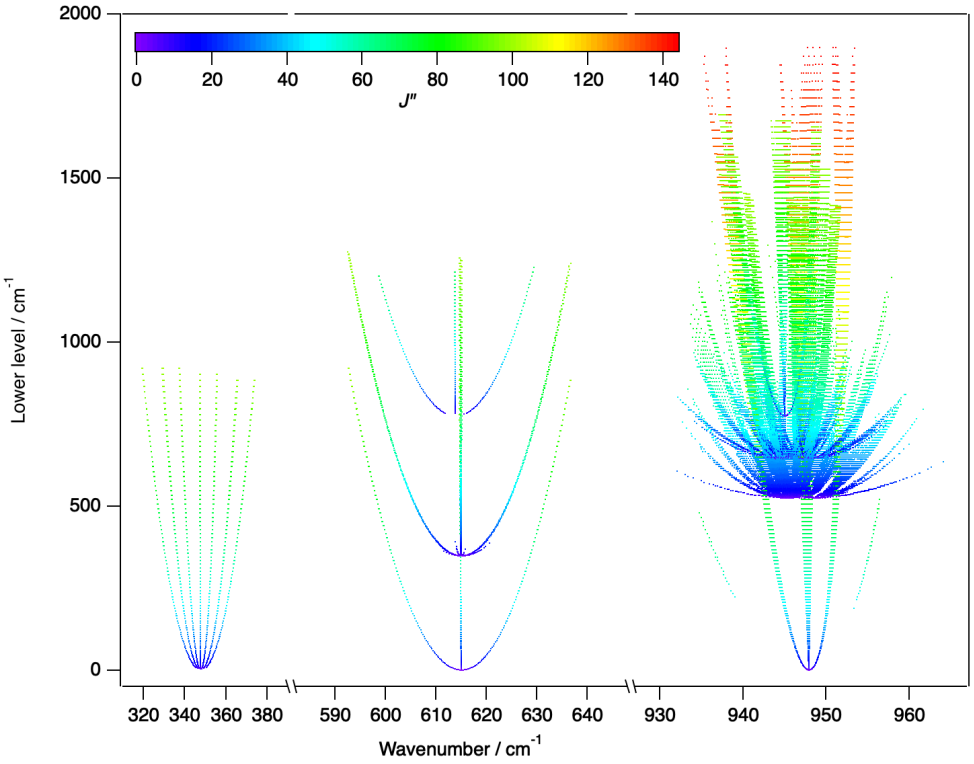

Figure 7: Representation of the lower level wavenumber for all transitions present in the SHeCaSDa database. Colors are used to display the lower state rotational quantum number value, J''.

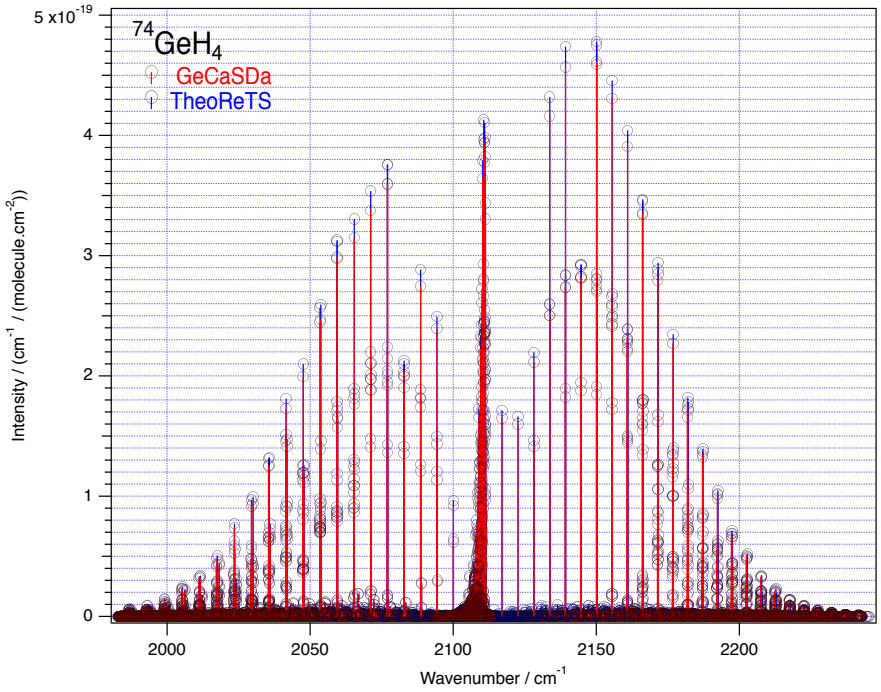

Figure 8: Comparison of the GeCaSDa and TheoReTS databases in the region of the intense ν_3 stretching band of $^{74}GeH_4$.

Table 7: Rovibrational transitions in RuCaSDa. The polyad sheme is described by the (i_1; i_2; ...; i_N) multiplet as explained in section 2.1.

Transitions	Nb. dipolar	Dipolar wavenumber cm^{-1}	Dipolar intensity $cm^{-1}/(molecule\ cm^{-2})$
$^{97}RuO_4$			
Scheme 1 (0,0,1,0)			
$P_1 - P_0$	3345	898 – 948	1×10^{-23} – 1×10^{-20}
$^{98}RuO_4$			
Scheme 1 (0,0,1,0)			
$P_1 - P_0$	3345	897 – 947	1×10^{-23} – 1×10^{-20}
$^{99}RuO_4$			
Scheme 1 (0,0,1,0)			
$P_1 - P_0$	3347	896 – 947	8×10^{-24} – 1×10^{-20}
$^{100}RuO_4$			
Scheme 1 (0,0,1,0)			
$P_1 - P_0$	3350	895 – 946	8×10^{-24} – 1×10^{-20}
$^{101}RuO_4$			
Scheme 1 (0,0,1,0)			
$P_1 - P_0$	3352	894 – 945	8×10^{-24} – 1×10^{-20}
$^{102}RuO_4$			
Scheme 1 (0,0,1,0)			
$P_1 - P_0$	3354	893 – 944	8×10^{-24} – 1×10^{-20}
$^{103}RuO_4$			
Scheme 1 (0,0,1,0)			
$P_1 - P_0$	3361	893 – 944	8×10^{-24} – 1×10^{-20}
$^{104}RuO_4$			
Scheme 1 (0,0,1,0)			
$P_1 - P_0$	3364	892 – 943	8×10^{-24} – 1×10^{-20}
$^{106}RuO_4$			
Scheme 1 (0,0,1,0)			
$P_1 - P_0$	3387	890 – 941	8×10^{-24} – 1×10^{-20}
Total	30 205		

Table 8: Rovibrational transitions in TFSiCaSDa. The polyad sheme is described by the (i_1; i_2; ...; i_N) multiplet as explained in section 2.1.

Transitions	Nb. dipolar	Dipolar wavenumber cm^{-1}	Dipolar intensity cm^{-1}/(molecule cm^{-2})
$^{28}SiF_4$			
Scheme 1 (0,0,1,0)			
$P_1 - P_0$	17 139	1010 – 1049	8×10^{-24} – 2×10^{-20}
$^{29}SiF_4$			
Scheme 1 (0,0,1,0)			
$P_1 - P_0$	23 660	1000 – 1041	8×10^{-24} – 2×10^{-20}
$^{30}SiF_4$			
Scheme 1 (0,0,1,0)			
$P_1 - P_0$	22 269	993 – 1032	8×10^{-24} – 2×10^{-20}
Total	63 068		

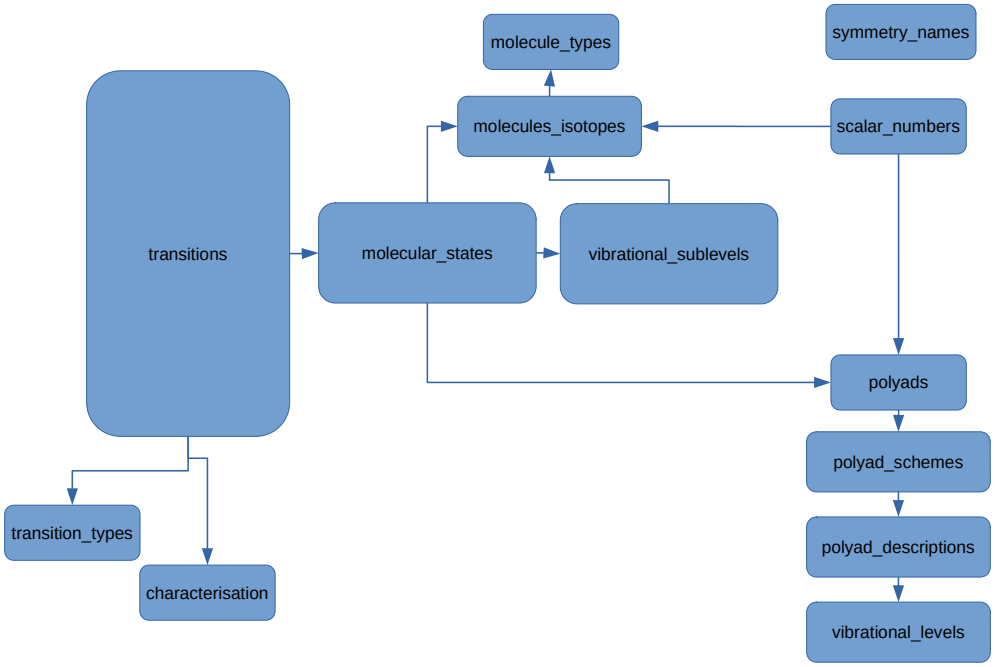

Figure 9: Simplified relational schema of the CaSDa databases. More information are given in Ref. [7].

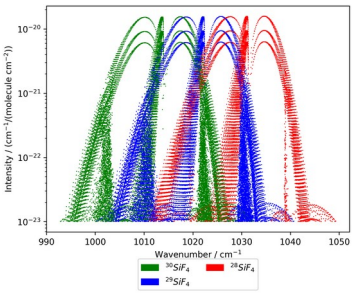

We present an important update of our previously existing calculated spectroscopic databases (CH_4 and C_2H_4), as well as new databases built on the same model (CF_4, SF_6, GeH_4, RuO_4 and SiF_4).